AD-A186 330 A COMPOSITE GRATING FOR MOIRE INTERFEROMETRY(U) 1/1
WSSHINGTON UNIV SEATTLE DEPT OF MECHANICAL ENGINEERING
F X WANG ET AL JUL 87 UWA/DME/TR-87/57
UNCLASSIFIED N00014-85-K-0187 F/G 20/6 NL

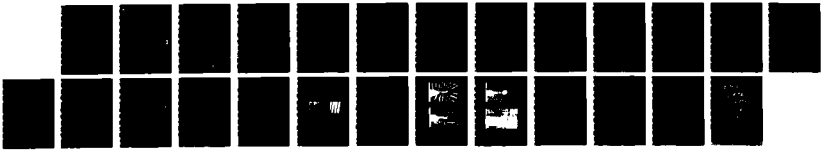

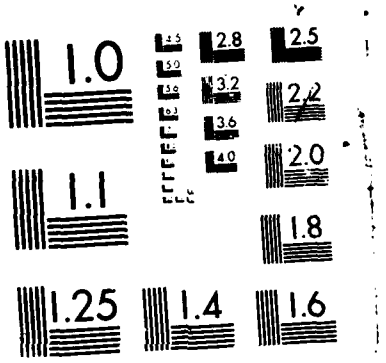

Office of Naval Research

Contract N00014-85-K-0187

Technical Report No. UWA/DME/TR-87/57

A COMPOSITE GRATING FOR MOIRE INTERFEROMETRY

by

F.X. Wang, B.S.-J. Kang and A.S. Kobayashi

July 1987

The research reported in this technical report was made possible through support extended to the Department of Mechanical Engineering, University of Washington, by the Office of Naval Research under Contract N00014-85-K-0187. Reproduction in whole or in part is permitted for any purpose of the United States Government.

Department of Mechanical Engineering

College of Engineering

University of Washington

A COMPOSITE GRATING FOR MOIRE INTERFEROMETRY

F.X. Wang*, B. S.-J. Kang**, and A.S. Kobayashi***

* Department of Aeronautics & Astronautics
**Department of Mechanical Engineering
University of Washington, Seattle, WA 98195

ABSTRACT

The theoretical background and the experimental verification of a new composite grating with two different grating densities, which was developed for simultaneous small and large displacement measurements of a single specimen using moire interferometry, are presented in this paper. A composite grating with line densities of 1200 and 300 lines/mm is then used to study the changes in the displacement field and the approximate J-integral values of a 5052-H32 aluminum, single edge notched (SEN) specimen under increasing load.

KEY WORDS

Moire Interferometry, Composite Grating, Elastic-plastic Fracture Mechanics

---

* Visiting Scientist, Department of Aeronautics and Astronautics, University of Washington, Seattle, Washington 98195.
** Assistant Professor, Department of Mechanical Engineering, West Virginia University, Morgantown, WV 26505.
*** Professor, Department of Mechanical Engineering, University of Washington 98195.

1. INTRODUCTION

Moire interferometry is capable of full field, in-plane as well as out-of-plane surface displacement measurements of elastic, inelastic and anisotropic materials. This experimental technique became more useful when Post and his associates [1,2,3] developed practical methods for producing the needed high density grating and for transferring the grating onto a specimen. The Post's method as well as other methods [4,5,6] have been used successfully to analyze various static plane problems in fracture mechanics. The high sensitivity in measuring the surface displacement by moire interferometry also was used by two of the authors who studied the crack tip field in ductile fracture specimens [7,8]. However, our study was hampered by the increasing magnitude of the displacements which eventually obliviated the moire fringes near the crack tip as the applied load was increased. A composite grating with two different grating frequencies of f_1 and f_2, either of which can be used as the active grating frequency, was thus developed to overcome this experimental difficulty. Using this composite grating, the sensitivity of the moire interferometry system can be selectively chosen where active grating of high frequency can be used during the earlier loading stage to measure the small surface deformation followed by the use of a low frequency active grating during the latter loading stage to measure the large surface deformations. In the following, the theoretical background and the procedures for producing and using this composite grating are present. Finally, the utility of the composite grating is demonstrated by estimating the J-intergral values in a 5052-H32 aluminum, single edge notched specimen which was loaded to failure.

2. THEORY

2.1 Superposition of Two Parallel Sine Gratings with Different Grating Frequencies

The grating functions for two parallel sine gratings, one with a grating frequency of f_1 and the other with a grating frequency of f_2, as shown in Figure 1, are

$$T_1(x) = t_o + t_1 \sin 2\pi f_1 x$$
$$T_2(x) = t'_o + t'_1 \sin 2\pi f_2 x \qquad (1)$$

where t_o, t'_o, t_1, and t'_1 are the linear developing coefficients, and f_1 and f_2 are the spatial frequencies of the gratings. A composite sine grating, which contains two different grating frequencies, f_1 and f_2, can be constructed by a double exposure technique. The resultant composite sine grating function is

$$T(x) = T_1(x) * T_2(x)$$
$$= \Big[t_o t'_o + t_1 t'_o \sin 2\pi f_1 x + t_o t'_1 \sin 2\pi f_2 x \qquad (2)$$
$$+ \tfrac{1}{2} t_1 t'_1 \sin 2\pi (f_1 - f_2) x + \tfrac{1}{2} t_1 t'_1 \sin 2\pi (f_1 + f_2) x \Big]$$

2.2 Diffraction Field of Parallel Composite Sine Grating

Consider a laser beam in the x-z plane entering perpendicularly to the composite sine grating as shown in Figure 2. The diffraction field appearing in the frequency plane is the convolution of the two individual fourier

transform planes of grating frequencies of f_1 and f_2. The diffraction field can be described as

$$\sin\theta = \begin{cases} 0 & 0 \text{ diffraction order} \\ \pm f_1\lambda & \pm 1 \text{ diffraction order} \\ \pm f_2\lambda & \pm 1 \text{ diffraction order} \\ \pm(f_1-f_2)\lambda & \pm 1 \text{ diffraction order} \\ \pm(f_1+f_2)\lambda & \pm 1 \text{ diffraction order} \end{cases} \quad (3)$$

where θ is the diffraction angle. If the laser beam in the x-z plane enters the composite sine grating with an incident angle of ϕ with respect to the z-axis, then

$$\sin\theta = \begin{cases} 0 + \sin\phi & 0 \text{ diffraction order} \\ \pm f_1\lambda + \sin\phi & \pm 1 \text{ diffraction order} \\ \pm f_2\lambda + \sin\phi & \pm 1 \text{ diffraction order} \\ \pm(f_1-f_2)\lambda + \sin\phi & \pm 1 \text{ diffraction order} \\ \pm(f_1+f_2)\lambda + \sin\phi & \pm 1 \text{ diffraction order} \end{cases} \quad (4)$$

2.3 Superposition of Two Perpendicular Sine Gratings with Different Grating Frequencies

The grating function for an orthogonal composite sine grating with frequencies, f_1 and f_2, as shown in Figure 3, is easily derived in a similar procedure as

$$T(x,y) = T_1(x) * T_2(y)$$

$$= \left[t_o t_1' + t_1 t_o' \sin 2\pi f_1 x + t_o t_1' \sin 2\pi f_2 y \right.$$

$$\left. + \frac{1}{2} t_1 t_1' \sin 2\pi (f_1 x - f_2 y) + \frac{1}{2} t_1 t_1' \sin 2\pi (f_1 x + f_2 y) \right] \qquad (5)$$

2.4 Diffraction Field of Orthogonal Composite Sine Grating

The diffraction field at the frequency plane due to a laser beam in the z plane entering perpendicularly to an orthogonal composite sine grating, as shown in Figure 4, can be described as

$$(\sin\theta, \sin\theta) = \begin{cases} (0,0) & 0 \text{ diffraction order} \\ (\pm f_1\lambda, 0) & \pm 1 \text{ diffraction order} \\ (0, \pm f_2\lambda) & \pm 1 \text{ diffraction order} \\ (\pm f_1\lambda, \pm f_2\lambda) & \text{cross } \pm 1 \text{ diffraction order} \end{cases} \qquad (6)$$

In general, if a laser beam in the x-z plane enters the orthogonal composite sine grating at an incident angle of ϕ with respect to the z-axis, then

$$(\sin\theta, \sin\theta) = \begin{cases} (0,0) + (\sin\phi, 0) & 0 \text{ diffraction order} \\ (\pm f_1\lambda, 0) + (\sin\phi, 0) & +1 \text{ diffraction order} \\ (0, \pm f_2\lambda) + (\sin\phi, 0) & \pm 1 \text{ diffraction order} \\ (\pm f_1\lambda, \pm f_2\lambda) + (\sin\phi, 0) & \text{cross } \pm 1 \text{ diffraction order} \end{cases} \qquad (7)$$

2.5 Moire Interferometry with Composite Grating as Specimen Grating

Now consider a moire interferometry system which contains two gratings, a reference grating and a specimen grating, as shown in Figure 5. Let a parallel composite grating be the specimen grating and denote the grating frequency of

the reference grating as f^*. Let the incident angle, ϕ, in Figure 5, satisfy the following condition of

$$\sin\phi = \frac{\lambda}{2} f^* \tag{8}$$

Equation (8) represents the condition for generating symmetrical zero and first diffraction orders from the reference grating. These rays will generate the moire fringes upon interfering with the specimen grating. With the composite grating as the specimen grating, the sensitivity of the moire fringe can be chosen with different reference grating frequencies, f^*, as follows:

$$\begin{aligned} f^* &= 2f_1 \quad \rightarrow \quad u = N/f_1 \\ f^* &= 2f_2 \quad \rightarrow \quad u = N/f_2 \\ f^* &= 2(f_1-f_2) \quad \rightarrow \quad u = N/(f_1-f_2) \\ f^* &= 2(f_1+f_2) \quad \rightarrow \quad u = N/(f_1+f_2) \end{aligned} \tag{9}$$

where u represents the displacement field generated by moire interferometry and N is the moire fringe number.

3. PRODUCTION OF COMPOSITE GRATING

Figure 6 shows the optical setup, which is similar to that of Ref. [3], for producing the composite grating of frequencies of f_1 and f_2. In this investigation, a 1200/300 lines/mm composite grating was chosen. First, a virtual grating of frequency of f=300 lines/mm was produced and recorded on a photographic plate (Kodak High Resolution Plate, type TE). An argon ion laser with 150 mW power setting was used with an exposure time of 0.2 seconds. The optical setup was then changed to a virtual frequency grating of f=1200

lines/mm and the photographic plate was exposed again with a laser power setting of 500 mW and an exposure time of 0.4 seconds. The exposed plate was developed (Kodak developer, D-19 for 5 minutes), fixed and bleached. The final step prior to drying is to dip the plate in a wetting agent (Kodak Photo-Flo, diluted to 200:1). This developing procedure was essentially identical to that discussed in Ref. [2].

4. MOIRE INTERFEROMETRY USING COMPOSITE GRATING

The optical setup, which was used to generate moire fringes is shown in Figure 7 in which two virtual reference gratings of frequencies 2400 and 600 lines/mm were used. This arrangement corresponds to a fringe multiplication of two or $f^{*}=2f_2$ and $f^{*}=2f_1$ in Equation (9), where f_2=1200 lines/mm and f_1=300 lines/mm. A 1200/300 lines/mm parallel composite grating was then inserted in the specimen grating location. Figure 8 shows two in-plane rotation moire patterns produced by the 1200/300 lines/mm composite grating with 0.06 degrees in-plane rotation. As shown in Figure 8, the ratio of the fringe density coincides with the theoretical prediction of 4:1.

5. STABLE CRACK GROWTH IN 5052-H32 SEN SPECIMEN

A fatigue precracked 5052-H32 aluminum single edge notch (SEN) specimen, as shown in Figure 9, was tested for stable crack growth to failure. With no load on the specimen, the mirror for virtual grating in Figure 7 was first adjusted for the initial null fields at the two virtual reference grating frequencies of 2400/600 lines/mm. The light paths of the two virtual reference gratings are controlled by two shutters. At each loading stage, moire fringe

patterns corresponding to either 2400 lines/mm or 600 lines/mm of the reference grating frequencies were selectively recorded. Figure 10 and 11 shows two moire fringe patterns for virtual reference grating frequencies of 2400 lines/mm and 600 lines/mm, at the first and fourth level of applied load, respectively. The ratio of the two fringe densities between the two moire patterns coincides with the theoretical prediction of 4:1.

The moire fringe pattern, which was generated by the denser 2400 line/mm virtual grating, at the fourth level of applied load of 2.08 kN is almost indistinguishable and thus only the moire fringe patterns corresponding to the coarse virtual grating of 600 lines/mm were recorded in the subsequent seven load levels prior to rapid fracture.

Also shown in Figs. 10 and 11 is the rectangular contour used in estimating the J-integral using the procedure described in Refs. [7,8]. The J values estimated when testing a similar 5052-H32 SEN specimen to fracture [8] shows that the integration path used in this analysis was sufficiently far away from the fatigued crack tip, which was blunted by large scale yielding, and is outside of the path dependent region of J [9]. Figure 12 shows the estimated J resistance curve to rapid tearing, which was obtained by using the composite grating for the 5052-H32 SEN specimen.

5. DISCUSSIONS

For a composite grating of frequencies of f_1 and f_2, four active grating frequencies, f_1, f_2, (f_1+f_2) and (f_2-f_1), can be chosen as shown by Equation (9). With a 600/700 lines/mm composite grating, the ratio of the

sensitivities of the moire system can be as high as 13:1, i.e. 1300 lines/mm versus 100 lines/mm. Composite grating, is a very useful feature in the wide range of grating frequencies, which can be generated rapidly, for measuring the displacements near a ductile crack tip region with increasing load. Thus, using a composite grating, all phases of the increasing displacements can be recorded by the moire interferometry and thus, the measurable range of displacement field of a ductile fracture specimen is extended.

Application of the composite grating with moire interferometry is not restricted to measurement of a ductile crack tip displacement field. One useful application of moire interferometry with composite grating is to measure the displacement fields of a bonded dissimilar materials with large differences the rigidities of each material.

6. CONCLUSION

A new composite grating with two different grating densities has been developed. The theoretical background and the experimental verification of the composite grating are described. The utility of a composite grating is demonstrated by real-time moire interferometry test, where both small and large surface displacements of a single fracture specimen was recorded without changing the active/reference grating setup.

7. ACKNOWLEDGEMENT

The work reported here was completed under ONR Contract N00014-85-K-0187. The authors wish to acknowledge the support and encouragement of Dr. Yapa Rajapakse, ONR, during the course of this investigation.

8. REFERENCES

1. D. Post, Mechanics of Nondestructive Testing, edited by W.W. Stinchcomb, Plenum Publishing Corp., (1980).

2. D. Post, Optical Engineering, Vol. 21, No. 3, pp. 458-467, (1982).

3. D. Post, SEM Handbook on Experimental Mechanics, edited by A.S. Kobayashi, pp. 314-387, Prentice-Hall, (1987).

4. A. Ohta, M. Kosuge, and E. Sasaki, International Journal of Fracture, 13, 289 (1977).

5. C.A. Walker and J. McKelvie, Experimental Mechanics, 18(8), 316, (1978).

6. A. McDonach, J. McKelvie, P. MacKenzie, and C.A. Walker, Experimental Techniques, 23(2), 20, (June 1983).

7. B.S.-J. Kang, A.S. Kobayashi and D. Post, "Stable Crack Growth in Aluminum Tensile Specimens," to be published in Experimental Mechanics.

8. B.S.-J. Kang and A.S. Kobayashi, "J-resistance Curves in Aluminum SEN Specimens," to be published in Experimental Mechanics.

9. R.M. McMeeking, Journal of Mechanics and Physics of Solids, 25, 357, (1972).

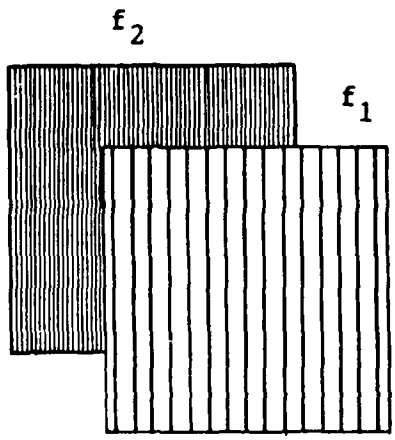

FIGURE 1 TWO PARALLEL SINE GRATINGS WITH DIFFERENT GRATING FREQUENCIES

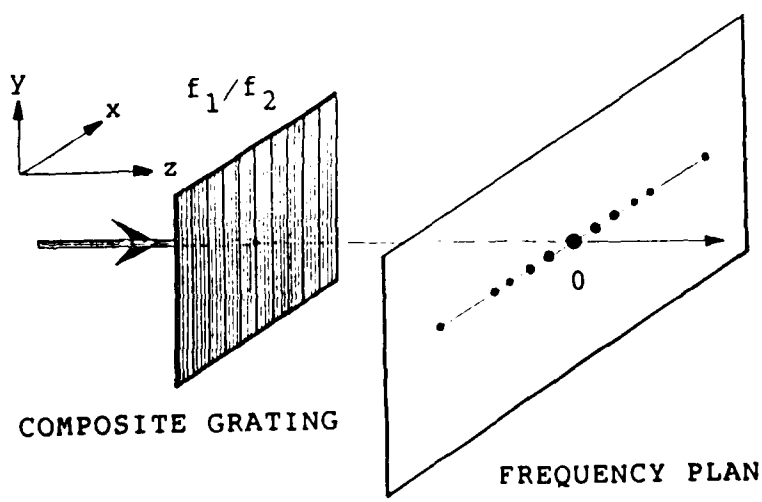

FIGURE 2 DIFFRACTION FIELD OF A PARALLEL COMPOSITE GRATING

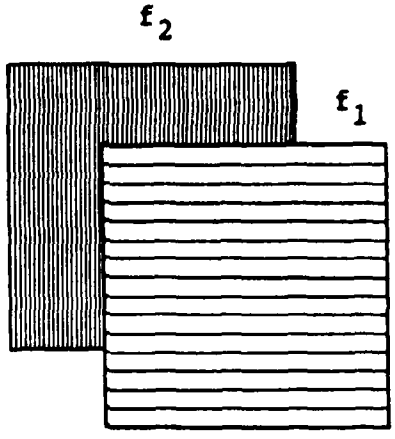

FIGURE 3 TWO PERPENDICULAR SINE GRATINGS WITH DIFFERENT GRATING FREQUENCIES

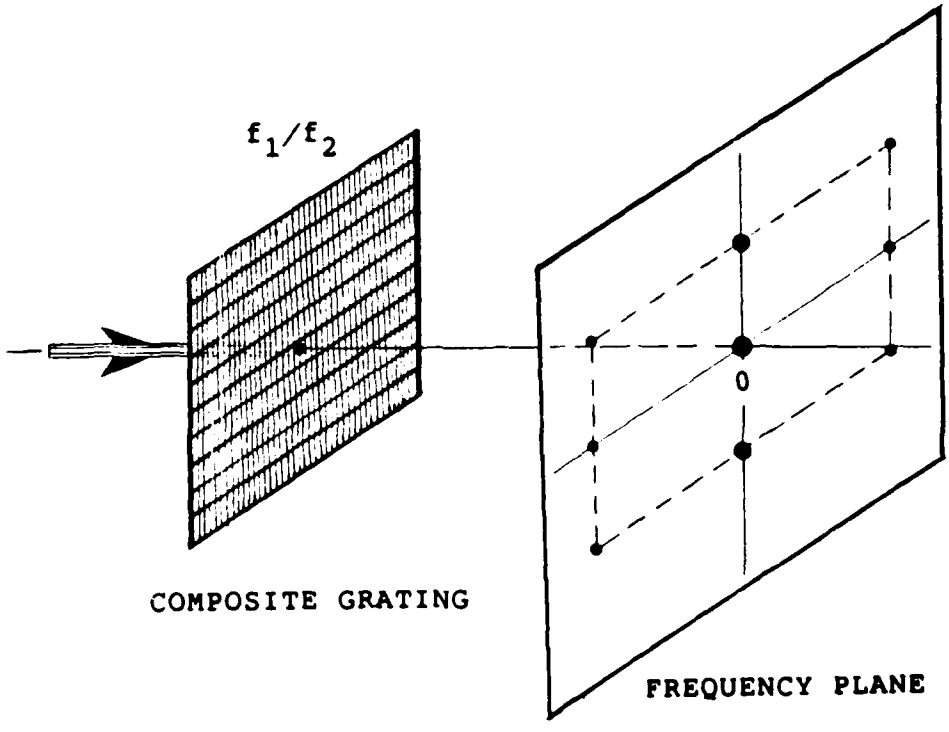

FIGURE 4 DIFFRACTION FIELD OF AN ORTHOGONAL COMPOSITE GRATING

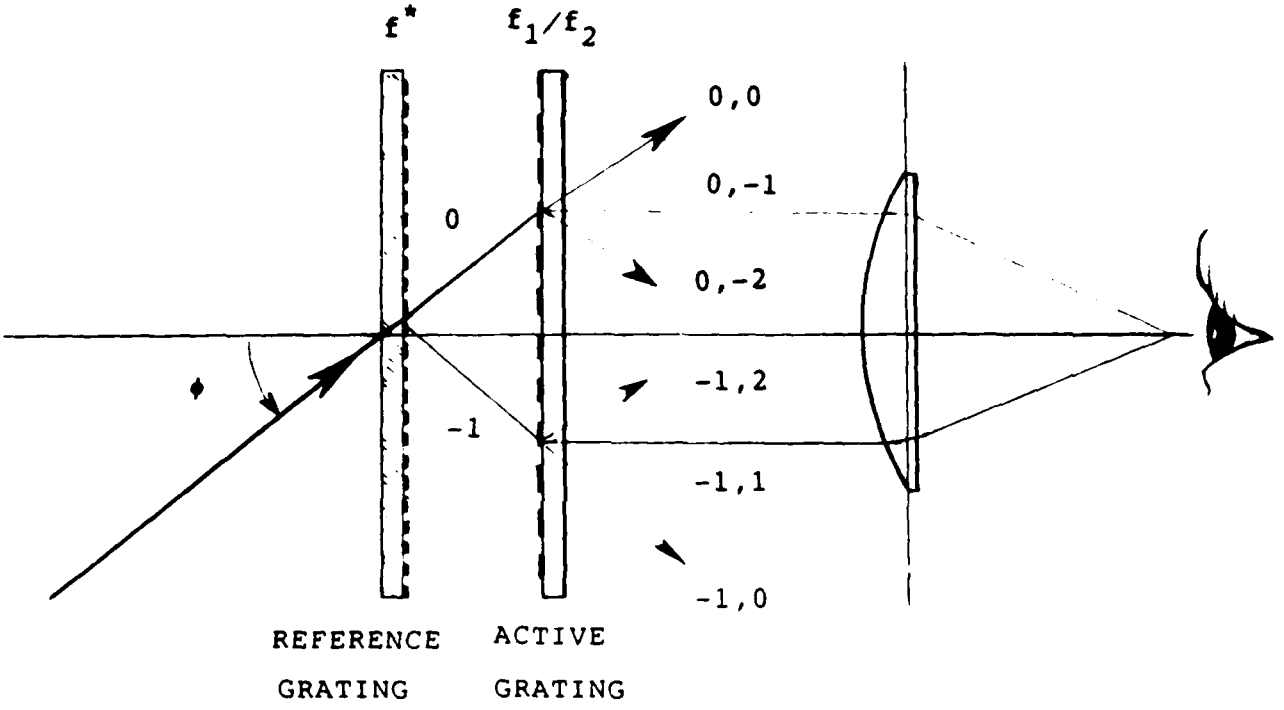

FIGURE 5 MOIRE INTERFEROMETRY WITH COMPOSITE GRATING AS THE ACTIVE GRATING

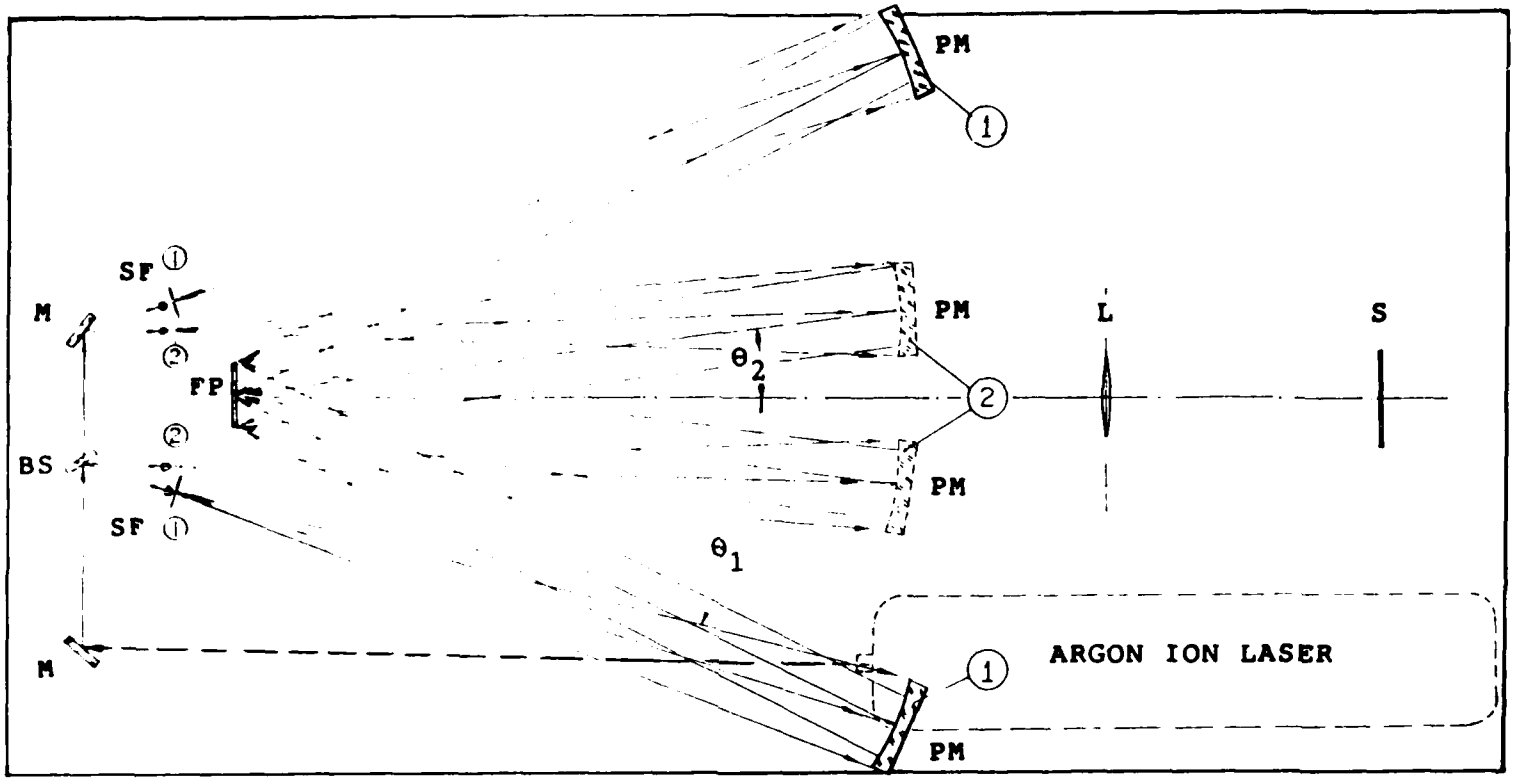

θ_1,θ_2: incident angles for virtual gratings of frequencies, f_1 and f_2,
BS: beam splitter, FP: film plate, L: lens, M: mirror,
PM: parabolic mirror, SF: spatial filter, S: screen,

FIGURE 6 OPTICAL SETUP FOR PRODUCING COMPOSITE GRATING

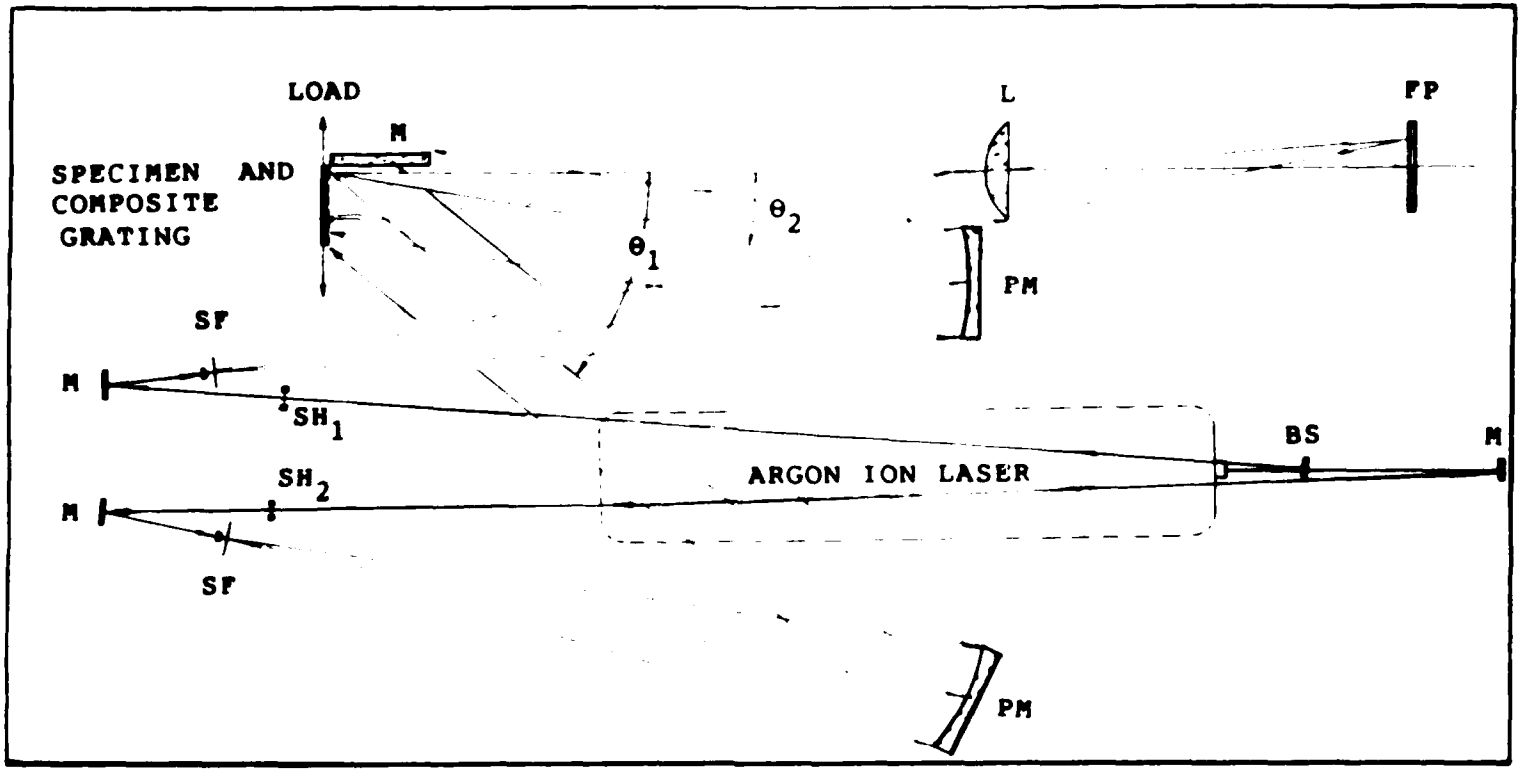

θ_1,θ_2: incident angles for virtual gratings of frequencies, f_1 and f_2,
BS: beam splitter, FP: film plate, L: lens, M: mirror,
PM: parabolic mirror, SF: spatial filter, SH: shutter.

FIGURE 7 OPTICAL SETUP FOR MOIRE INTERFEROMETRY WITH COMPOSITE GRATING

Active Grating Frequency
1200 lines/mm

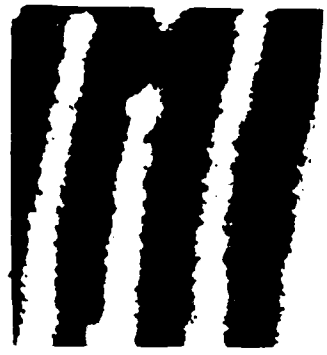

Active Grating Frequency
300 lines/mm

FIGURE 8 MOIRE FRINGES GENERATED BY COMPOSITE GRATING WITH IN-PLANE ROTATION OF 0.06 DEGREES

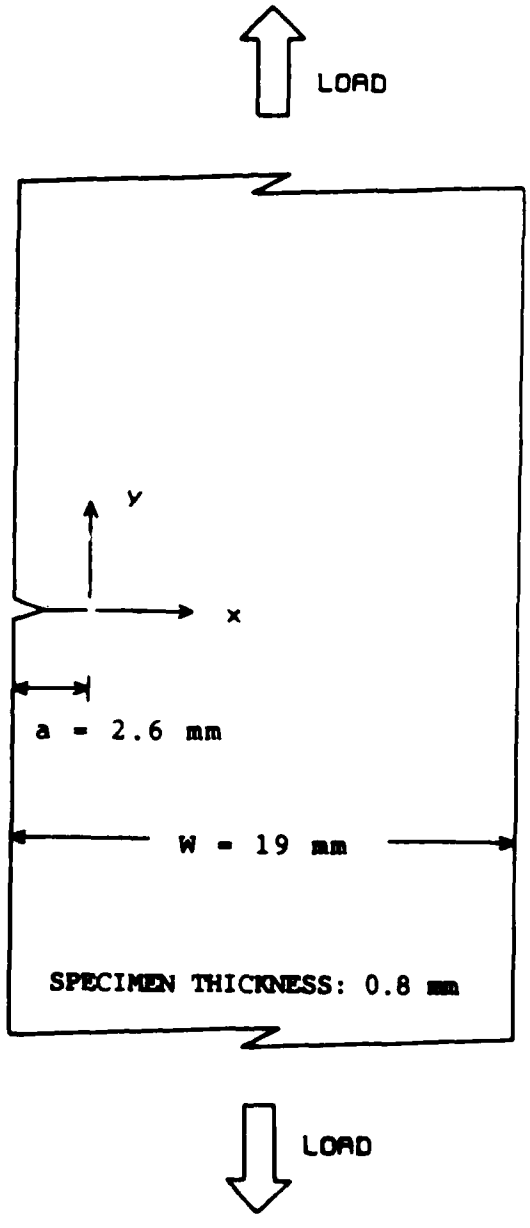

FIGURE 9 5052-H32 ALUMINUM SINGLE EDGE NOTCHED (SEN) SPECIMEN

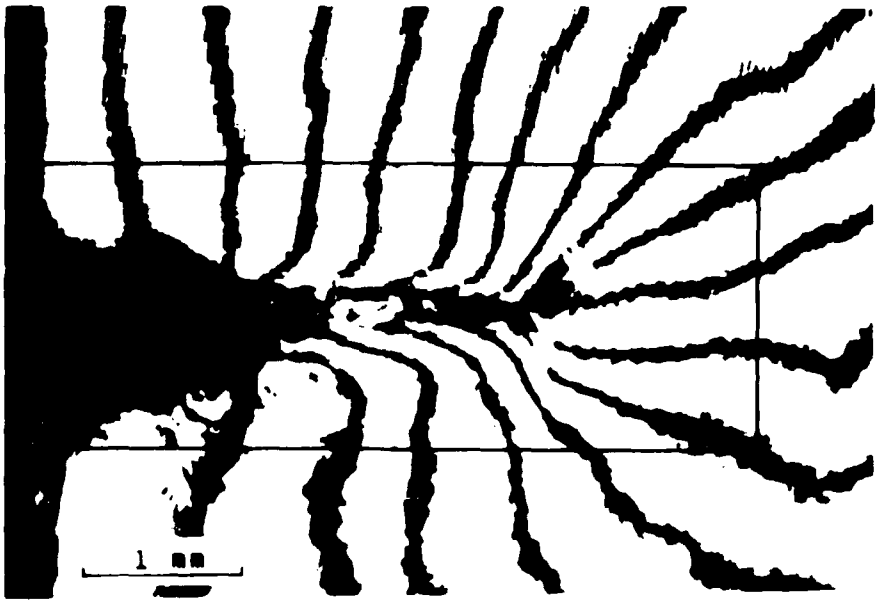

(Active Grating Frequency 300 lines/mm)

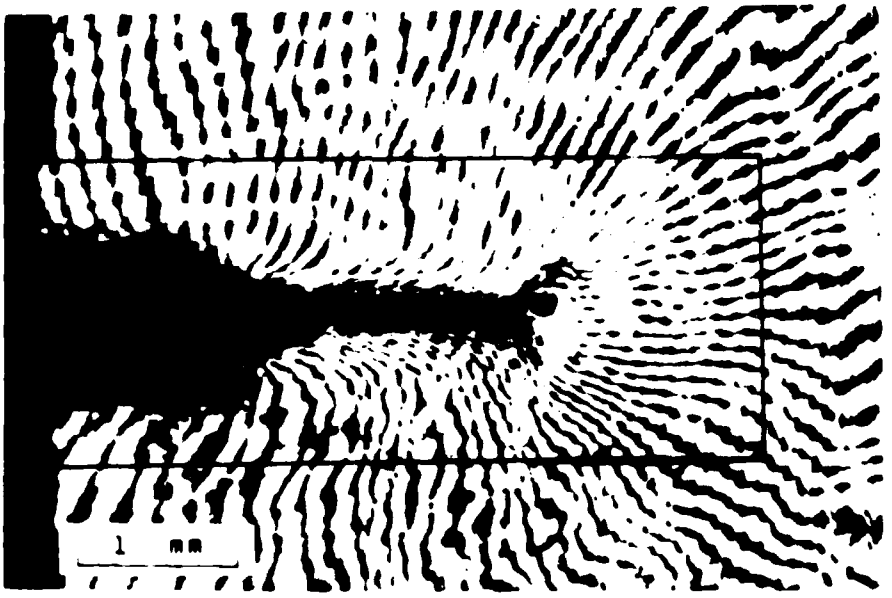

(Active Grating Frequency 1200 lines/mm)

FIGURE 10 MOIRE FRINGES GENERATED BY COMPOSITE GRATING AT APPLIED LOAD OF 1 22 KN

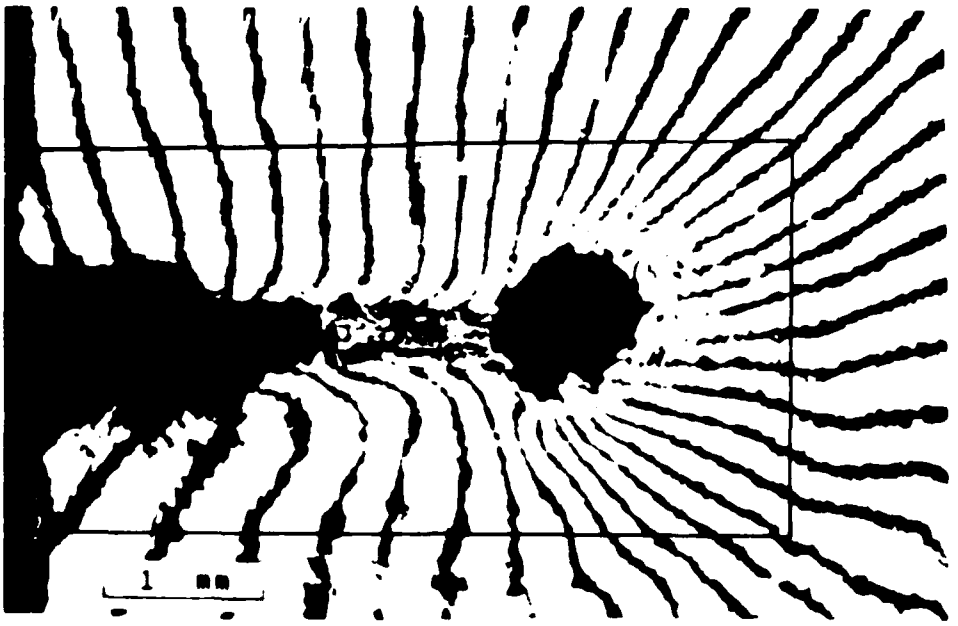

(Active Grating Frequency 300 lines/mm)

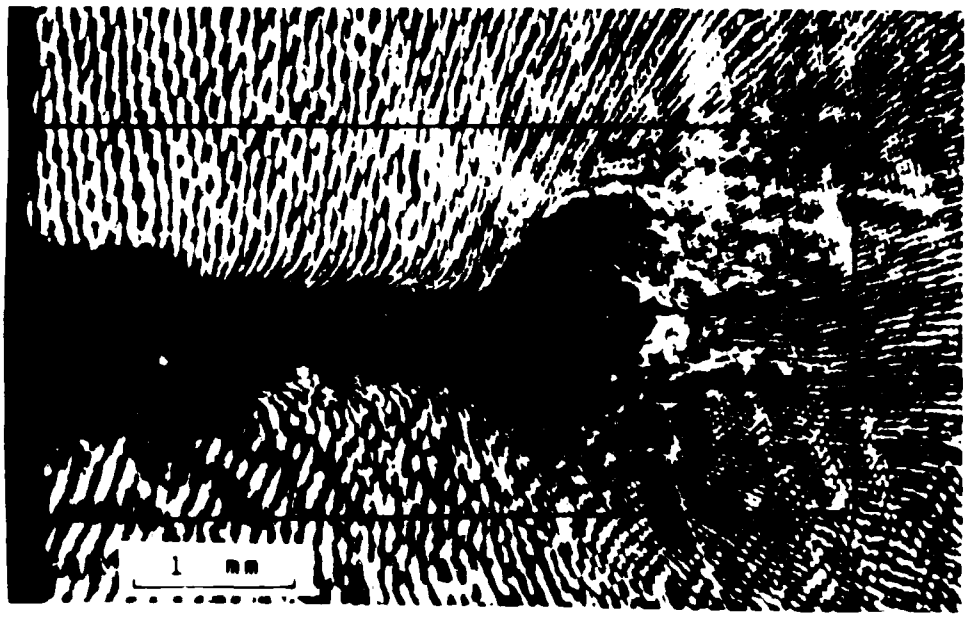

(Active Grating Frequency 1200 lines/mm)

FIGURE 11 MOIRE FRINGES GENERATED BY COMPOSITE GRATING AT APPLIED LOAD OF 2.08 KN

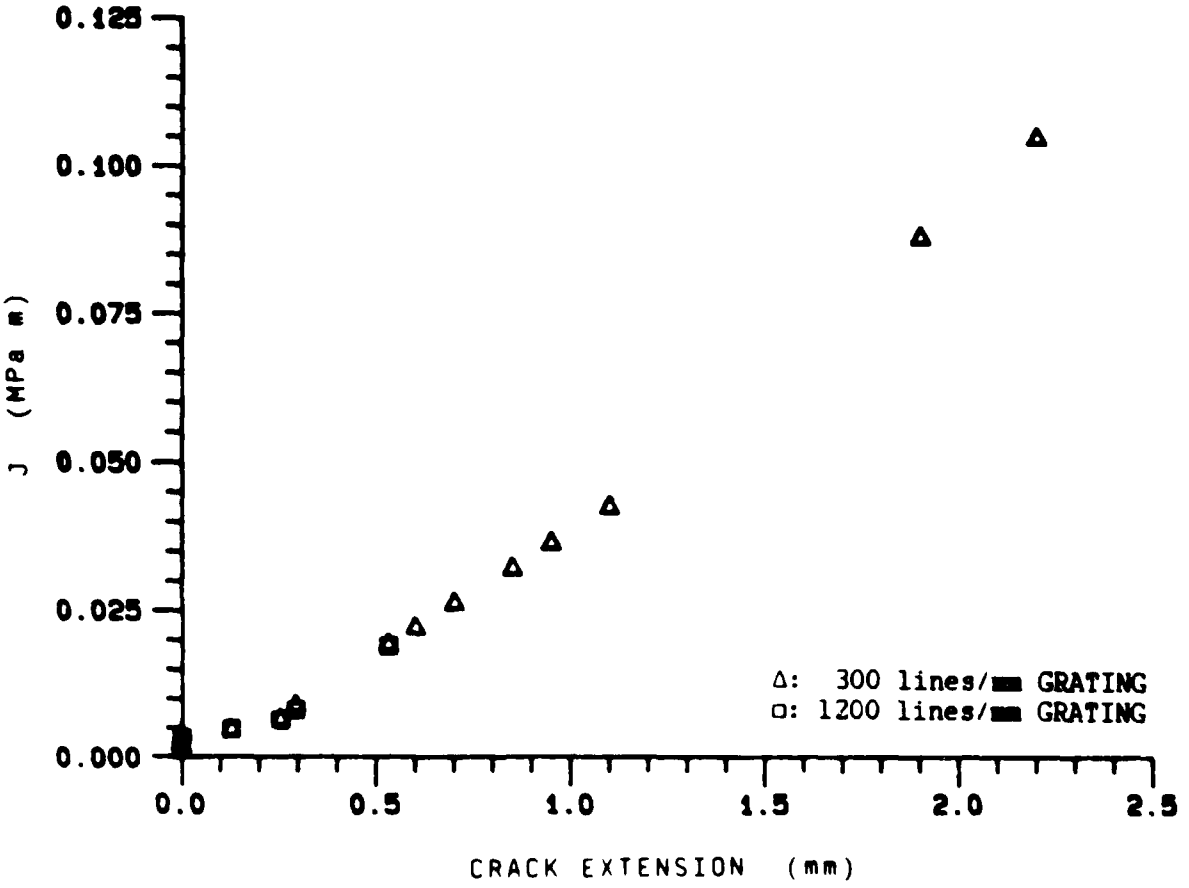

FIGURE 12 J VALUES VERSUS CRACK EXTENSION, 5052-H32 ALUMINUM SEN FATIGUE PRECRAKCED SPECIMEN WITH INITIAL CRACK LENGTH 2.94 mm, SPECIMEN NO. JCP1.

JHB MASTER MAILING LIST
UPDATED 7/86

Office of Naval Research
800 N. Quincy Street
Arlington, VA 22217-5000
Attn: Code 1132SM (6 copies)

Office of Naval Research
800 N. Quincy Street
Arlington, VA 22217-5000
Attn: Code 1131

Defense Documentation Center (4 copies)
Cameron Station
Alexandria, VA 22314

Naval Research Laboratory
Washington, DC 20375
Attn: Code 6000

Naval Research Laboratory
Washington, DC 20375
Attn: Code 6300

Naval Research Laboratory
Washington, DC 20375
Attn: Code 6380

Naval Research Laboratory
Washington, DC 20375
Attn: Code 5830

Naval Research Laboratory
Washington, DC 20375
Attn: Code 6390

Naval Research Laboratory
Washington, DC 20375
Attn: Code 2620

David W. Taylor Naval Ship
Research & Development Center
Annapolis, MD 21402
Attn: Code 28

David W. Taylor Naval Ship
Research & Development Center
Annapolis, MD 21402
Attn: Code 2812

David W. Taylor Naval Ship
Research & Development Center
Annapolis, MD 21402
Attn: Code 1814

David W. Taylor Naval Ship
Research & Development Center
Bethesda, MD 20084
Attn: Code 750

David W. Taylor Naval Ship
Research & Development Center
Bethesda, MD 20084
Attn: Code 2740

David W. Taylor Naval Ship
Research & Development Center
Bethesda, MD 20084
Attn: Code 2740.4

Naval Air Development Center
Warminster, PA 18974
Attn: Code 6043

Naval Air Development Center
Warminster, PA 18974
Attn: Code 6063

Naval Surface Weapons Center
White Oak, MD 20910
Attn: Code R33
Technical Library

Naval Surface Weapons Center
Dahlgren, VA 22448
Attn: Technical Library

Naval Ship Eng Center
Port Hueneme, CA 93043
Attn: Technical Library

Naval Underwater Systems Center
New London, CT 06320
Attn: Code 44
Technical Library

Naval Underwater Systems Center
Newport, RI 02841
Attn: Technical Library

Naval Weapons Center
China Lake, CA 93555
Attn: Technical Library

NRL/Underwater Sound Reference Det.
Orlando, FL 32856
Attn: Technical Library

Chief of Naval Operations
Department of the Navy
Washington, DC 20350
Attn: Code OP-098

Commander
Naval Sea Systems Command
Washington, DC 20362
Attn: Code 05R25

Commander
Naval Sea Systems Command
Washington, DC 20362
Attn: Code 05R26

Commander
Naval Sea Systems Command
Washington, DC 20362
Attn: Code 09B31

Commander
Naval Sea Systems Command
Washington, DC 20362
Attn: Code 55Y

Commander
Naval Sea Systems Command
Washington, DC 20362
Attn: Code 55Y2

Commander
Naval Air Systems Command
Washington, DC 20361
Attn: Code 930

Commander
Naval Air Systems Command
Washington, DC 20361
Attn: Code 7226

Commander
Naval Air Systems Command
Washington, DC 20361
Attn: Code 3104

Commander
Naval Air Systems Command
Washington, DC 20361
Attn: Code 310B

US Naval Academy
Mechanical Engineering Dept.
Annapolis, MD 21402

Naval Postgraduate School
Monterey, CA 93940
Attn: Technical Library

Mr. Jerome Persh
Staff Specialist for Matls & Struct
OUSDR&E The Pentagon
Room 3D1089
Washington, DC 20301

Professor J. Hutchinson
Harvard University
Div of Applied Sciences
Cambridge, MA 02138

Professor B.M. Gallagher
Worcester Polytechnical Institute
Worcester, MA 01609

Dr. Harold Liebowitz, Dean
School of Engr & Applied Sci
George Washington University
Washington, DC 20052

Professor T.F. Mann
Vanderbilt University
Dept of Mech & Matls Engr
Nashville, TN 37235

Professor Albert S. Kobayashi
Dept of Mechanical Engineering
University of Washington
Seattle, WA 98195

Professor L.B. Freund
Brown University
Division of Engineering
Providence, RI 02912

Professor B. Budiansky
Harvard University
Division of Applied Sciences
Cambridge, MA 02138

Professor S.M. Arnold
Georgia Institute of Technology
School of Engr & Mechanics
Atlanta, GA 303

Professor J. Duffy
Brown University
Div of Engineering
Providence, RI 02912

Professor J.D. Achenbach
Northwestern University
Dept of Civil Engineering
Evanston, IL 60201

Professor F.A. McClintock
Dept of Mechanical Engineering
Massachusetts Institute of Technology
Cambridge, MA 02139

Professor J.M. Paros
Dept of Mechanical Engineering
Massachusetts Institute of Technology
Cambridge MA 02139

Dr. M.F. Hamilton
Southwest Research Institute
PO Drawer 28510
6220 Culebra Road
San Antonio, TX 78284

Professor F.P. Chiang
Dept of Mechanical Engr
State U of NY at Stony Brook
Stony Brook, New York 11794

Professor S.S. Wang
Dept of Theoretical & Applied Mechs
University of Illinois
Urbana, Illinois 61801

Professor [illegible]
Civil Engr Department
Texas A&M University
College Station, Texas 77843

Professor I.M. Daniel
Dept of Mechanical Engr
Illinois Institute of Technology
Chicago, Illinois 60616

Professor C.T. Sun
School of Aeronautics & Astronautics
Purdue University
W. Lafayette, IN 47907

Professor J. Auerbach
Dept of Mech Engr & Mechanics
Drexel University
Philadelphia, PA 19104

Professor T.H. Lin
University of California
Civil Engineering Dept
Los Angeles, California 90024

Professor J.L. Sverdrup
Dept of Civil Engr
Rensselaer Polytechnic Institute
Troy, New York 12180

Dr. R.M. Christensen
Chemistry & Matls Sci Dept
Lawrence Livermore National Laboratory
PO Box 808
Livermore, CA 94550

Professor J.R. Rice
Division of Applied Sciences
Harvard University
Cambridge, MA 02138

Professor W.M. Sharpe
The Johns Hopkins University
Dept of Mechanics
Baltimore, MD 21218

Professor L.F. Shin
Brown University
Division of Engineering
Providence, RI 02912

Professor A. Rosakis
California Institute of Tech
Graduate Aeronautical Laboratories
Pasadena, CA 91125

Professor D. Post
VA Polytechnic & State U
Dept of Engr Science & Mechanics
Blacksburg, VA 24061

Professor W. Sachse
Cornell University
Dept of Theoretical
& Applied Mechanics
Ithaca, NY 14853

Professor G.S. Springer
Stanford University
Dept of Aeronautics & Astronautics
Stanford, CA 94305

Professor M.T. Hahn
Washington University
Center for Composites Research
St. Louis, MO 63130

Professor S.K. Datta
University of Colorado
Dept of Mechanical Engineering
Boulder, CO 80309

Dr. M.L. Williams
School of Engineering
University of Pittsburgh
Pittsburgh, PA 15261

Dr. R.M. Gallagher
VP & Dean of Faculty
Worchester Polytechnic Institute
Worchester, MA 01609

Dr. D.C. Drucker
Dept of Aerospace Eng & Mechanics
University of Florida
Tallahassee, FL 32611

Dean B.A. Boley
Dept of Civil Engineering
Northwestern University
Evanston, IL 60201

master list + 1dm107
July 24, 1986

Unclassified

SECURITY CLASSIFICATION OF THIS PAGE (When Data Entered)

REPORT DOCUMENTATION PAGE		READ INSTRUCTIONS BEFORE COMPLETING FORM
1. REPORT NUMBER UWA/DME/TR-37/57	2. GOVT ACCESSION NO. ADA186330	3. RECIPIENT'S CATALOG NUMBER
4. TITLE (and Subtitle) A Composite Grating for Moire Interferometry		5. TYPE OF REPORT & PERIOD COVERED Technical Report
		6. PERFORMING ORG. REPORT NUMBER UWA/DME/TR-87/57
7. AUTHOR(s) F.X. Wang, B.S.-J. Kang and A.S. Kobayashi		8. CONTRACT OR GRANT NUMBER(s) N00014-85-K-0187
9. PERFORMING ORGANIZATION NAME AND ADDRESS Department of Mechanical Engineering, FU-10 University of Washington Seattle, Washington 98195		10. PROGRAM ELEMENT, PROJECT, TASK AREA & WORK UNIT NUMBERS
11. CONTROLLING OFFICE NAME AND ADDRESS Office of Naval Research Arlington, Virginia 22217		12. REPORT DATE July 1987 13. NUMBER OF PAGES 23
14. MONITORING AGENCY NAME & ADDRESS(if different from Controlling Office)		15. SECURITY CLASS. (of this report) Unclassified 15a. DECLASSIFICATION/DOWNGRADING SCHEDULE

16. DISTRIBUTION STATEMENT (of this Report)

Unlimited

17. DISTRIBUTION STATEMENT (of the abstract entered in Block 20, if different from Report)

18. SUPPLEMENTARY NOTES

19. KEY WORDS (Continue on reverse side if necessary and identify by block number)

Moire Interferometry, Composite Grating, Elastic-plastic Fracture Mechanics

20. ABSTRACT (Continue on reverse side if necessary and identify by block number)

The theoretical background and the experimental verification of a new composite grating with two different grating densities, which was developed for simultaneous small and large displacement measurements of a single specimen using moire interferometry, are presented in this paper. A composite grating with line densities of 1200 and 300 lines/mm is then used to study the changes in the displacement field and the approximate J-integral values of a 5052-H32 aluminum, single edge notched (SEN) specimen under increasing load.

DD FORM 1 JAN 73 1473 EDITION OF 1 NOV 65 IS OBSOLETE
S/N 0102-014-6601

Unclassified

SECURITY CLASSIFICATION OF THIS PAGE (When Data Entered)

END

DATE

FILMED

JAN

1988